Mining subsidence in a partially flooded abandoned mine: aseismic ground movement and consequences for post-mining risk management

Isabelle Contrucci, Cyrille Balland, Jannes Kinscher, Emmanuelle Klein

Mining Subsidence in a Partially Flooded Abandoned Mine: Aseismic Ground Movement and Consequences for Post-Mining Risk Management

I Contrucci *Ineris, France*

C Balland *Ineris, France*

J Kinscher *Ineris, France*

E Klein *Ineris, France*

Abstract

In the Lorraine area of eastern France, decades of iron-ore mining from 1850 to 1997 have left vast underground cavities beneath or near urban areas. Several major collapses occurred in the southern part of this iron-ore basin in the 1990s, after the mine closure and the flooding of underground mine workings. Following these large-scale collapses, the French government initiated a strategy of post-mining risk management to prevent and control risks associated with these ground failures. The high-risk zones are secured either by reducing the vulnerability while the moderate risk zones are monitored for public safety purposes by using in situ monitoring. This monitoring relies mainly on real-time microseismic systems, to detect precursors to a rapid large-scale collapse. Data recorded are processing automatically, and may generated alarm in case of abnormal evolution, in terms of number of event as well as in energy. A cell of expertise can be mobilized to analyse the situation and inform the local authorities of the evolutions of the situation. Evacuation can be triggered in case of danger for public safety.

After the progressive closing and then flooding of the northern iron basin ending in 2008, subsidence was observed in a town of the Lorrain basin in autumn of 2009. However, this local subsidence, with a low velocity of few centimeters per month, was not clearly detected by the borehole microseismic monitoring station located nearby. Only some microseismic events were recorded, which could not be unambiguously related to the beginning of the subsidence event. To better understand this lack of microseismic precursor a geophysical investigation was launched. A calibration blast experiment was carried out from a remaining old underground access in order to characterise the wave propagation properties in this context.

The results of this study show strong anelastic attenuation of the seismic waves though the monitored overburden most likely related to the extensive fault system intersecting the study site. Moreover, robbed pillar extraction and flooding of the site have induced a reduction of the mechanical properties of the overburden. These observations, added to a slow kinetics subsidence mechanism (~ cm/months) with little seismic energy release, may explain the lack of detected microseismicity during the subsidence event. In addition, low frequency microseismic events associated with the very slow subsiding movements might have not been detected by the used high frequency recording instruments, designed initially for rapid collapses (~ cm/hours).

Keywords: *microseismic; monitoring; post-mining risk; subsidence; anelastic attenuation; mine closure*

1 Introduction

In the Lorraine area in eastern France, decades of iron-ore mining from 1850 to 1997 have left vast underground chambers and pillars beneath urban areas. These residual voids are estimated to be 500 million m^3 in total size. Several major collapses occurred in the southern part of this iron-ore basin in the 1990s after the mine closure (Didier, 2007). These events happened a few months after the progressive rise of the water level in the underground workings, which was caused by the pumping stoppage of the mine water. Major and brutal collapses were provoked by the failure of residual abandoned underground pillars. Surface subsidence could reach two meters like in the Auboué area. More than five hundred buildings have been damaged due to these disorders and many had to be destroyed (Deck, 2002).

Following these large-scale collapses, the French government and the local authorities initiated a strategy of post-mining risk management to prevent and control the risks associated with these ground failures. By this strategy, first hazardous zones are identified, which is assessed by defining ranks according to their vulnerability and exposure of human infrastructure and activity. Then, the high risk zones are secured either by reducing the hazard or by surveying the hazard by means of microseismic monitoring (Bennani et al., 2003) The potential of the microseismic monitoring was assessed and validated in the geological context of the Lorrain basin by means of locally provoked small scaled mining collapses during the "Terres Rouges" experiment in 1997 (Couffin et al., 2003; Senfaute et al., 2000). Calibration blast were performed in the iron ore Lorrain basin to calibrate microseismic monitoring system (Contrucci et al., 2010) to adjust geophysical parameters.

So far no significant microseismic activity was recorded in the monitored areas that could be associated with the origin of a mining collapse. Nevertheless, a significant subsidence event was observed in a monitored town in the fall of 2009, located in the south-western edge of a flooded, abandoned chamber and pillar mining sector. For confidentiality reasons, the name of the site will remain anonymous. This local subsidence, with a velocity of several centimetres per month, was not fully detected by the microseismic monitoring station located nearby (Groseilliers station, Figure and Figure), only few events were recorded. We were then questioned about the reasons that led to this situation by undertaking thorough investigations on all of the measuring system and on microseismic wave propagation conditions on the site. No technical failure was highlighted by these investigations. However, the hypothesis of a gradual subsidence releasing low energy densities during the time became plausible based on results of the wave propagation modelling. Note that the area, affected by mining subsidence, is no longer accessible because of flooding of the area in late 2007. Among the hypotheses that may explain the lack of microseismic precursor and, given the kinetic of the phenomenon on several months, one is based on a large aseismic deformation of an overburden already deconsolidated. A second hypothesis is based on the local geophysical and geomechanical conditions affecting the effectiveness of the microseismic monitoring, like the faults corridor identified on the monitored area. A third hypothesis is based on an improper installation of the microseismic sensor in the borehole, and a bad coupling of the probe with the ground.

To explain the causes of this situation, a program of geophysical investigations was launched with a series of complementary operations to provide elements of response to the lack of microseismic detection. Calibration blasts were carried out from the eastern part of the accessible mine workings and additional sensors were deployed at the surface. This experimentation was carried out in September 2010. The aim of the experimentation, according to the hypothesis listed before, was to answer to the following questions: (1) What is the velocity and wave attenuation field? (2) What is the minimum source power that can be detected by the sensors? (3) What is the impact of the geology, the faults corridor and the integral pillar extraction zone on the wave propagation field ?

2 Context and Methods

The site shows many normal faults forming a corridor with an average orientation of about N45°. The main discontinuity of this system is a fault which is the northwest edge of the mine. The site has two areas of hazard (Figure), classified as risk of progressive subsidence. The iron ore layer was exploited with a recovery factor of about 47%. Operated by room and pillar method, mine workings are now flooded at the NGF level of ~ 208 m, and are located at about 160 m below the surface, with a dip of approximately 2.5° (NO). This configuration prevents to access to the area located directly below the collapsed region and below the Groseilliers microseismic station (Figure).

Cracks observed in the houses of the inhabitants of the town were observed in October 2009. This led to the establishment of a monthly levelling follow since December 2009 (Figure). The measured displacements reveal the formation of a basin whose maximum amplitude was 66 cm in April 2012. This basin is located south of the hazard zone. For this blast calibration experiment, different acquisition systems have been installed both on the surface and at bottom, in the mine, in addition to the permanent microseismic monitoring network stations named Lilas, Groseilliers (Figure). Two temporary geophones lines connected to two acquisition units were located at the surface. A temporary seismic network was installed inside the mine, consisting in two stations, each equipped with a geophone, a microphone, an hydrophone, a 3 components 1 Hz seismic station and a dynamic piezometer.

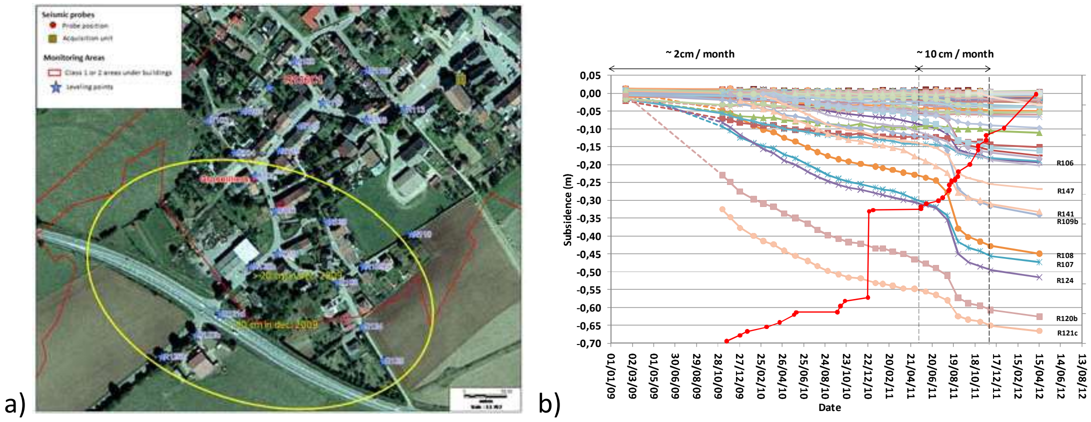

Figure 1 a) zoom on the subsided zone and location of the leveling points. Red line marks the limit of the risk zone, yellow line represents the extension of the surface subsidence (GEODERIS); b) leveling measurements since January 2009 until August 2012 (BRGM-DPSM) of the points located in figure a. Red curve represents the cumulative sensor energy of the microseismic events recoded during the period.

Figure shows the location of the different acquisition systems, blasts and rock falls performed for the experiment. The blasts were made in drilling of 5 meters depth and 60 mm of diameter. The explosive used was EURODYN 2000 dynamite type. These blasts were mainly located at the east of Lilas and Groseilliers stations, because of the mine flooding, although the basin subsidence is located to the South-West. Rock falls experiment (10 drops a weight of 500kg) was performed in the Louise gallery primarily to calibrate seismic and acoustic monitoring network located in the mine.

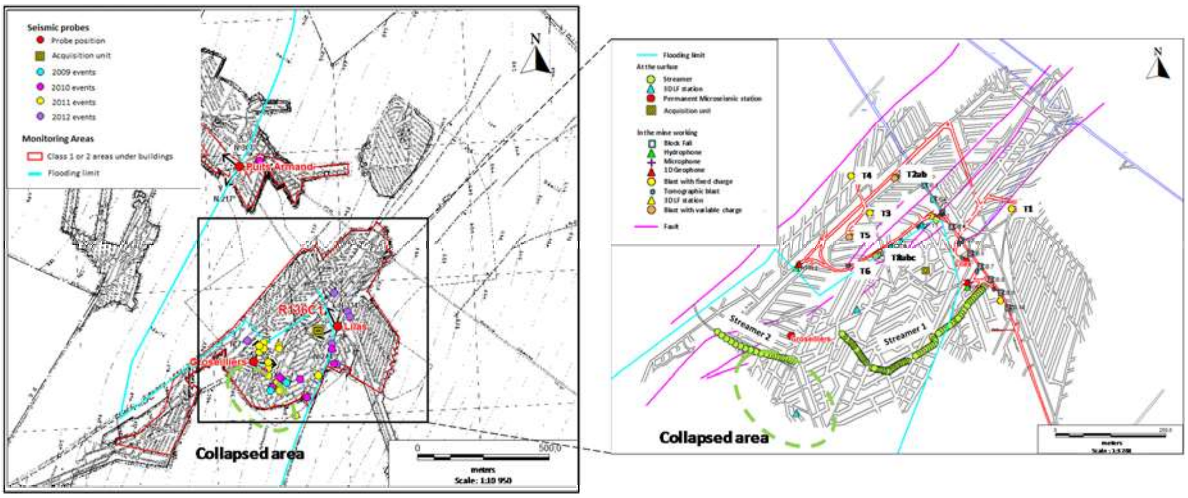

Figure 2 left map: mine workings of the iron ore grey layer of the site and location of the risk zone (red lines) and the permanent microseismic network (red points). Right map: Location of the different acquisition system and the blast superimposed to the grey layer mine workings (BRGM-DPSM)

To estimate the velocity field, two tools were used. The first tool is called SYTMISvel (Contrucci et al., 2010). It is able to build isotropic multilayer 1D velocity model by inversion. For the inversion input data are: P wave and/or S wave first arrival time, incident wave angle measured at 3 components seismic stations, number of geological layers, blast location and errors on arrival time picking and on angles. The second tool is called TOMSIS (software 2D seismic tomography (Balland et al., 2009)). In this case, the strata are not predefined. The propagation medium is discretized, which can account for the anisotropy of velocity. The anelastic wave attenuation was calculated by the spectral ratio approach (Sain et al., 2009; Toksoz et al., 1979). The spectral amplitude ratio was considered for collinear seismic rays of P waves with quasi vertical incidence angles emitted by weight drops of 500 kg, located just below the Lilas station.

3 Results

3.1 Velocity field

The first method of velocity estimation of the geological layers (Table 1) clearly shows a first low velocity layer of ~ 1900 m/s and ~ 30 m thick, which is located over a layer of ~ 3100 m/s of ~ 90 m thick. The third layer is ~ 30 m thick with a higher velocity of 3700 m/s. The last layer represents the mined layer with a velocity of ~ 3400 m/s. The first layer may be associated to both the altered layer and alternating marl-limestone while the second may be associated to the Bajocian limestone. Finally, the third layer is associated to marl of Charennes. Note that the velocity measurement integrates widely layers of smaller thickness as the layer of marl (19 m) located between two limestones, which give an idea of the limitations of the methods for estimating the seismic velocity in this context. Velocity observations are broadly consistent with what has been observed at other sites of iron basin (Contrucci et al., 2010; Tastet et al., 2007).

Table 1 : summary of the velocity characteristics of the model on the site.

Site		Surface	Bajocien	marl of Charennes	Iron layer
4 layers model	thickness [m]	27	89	33	40
	velocity [m/s]	1867	3137	3695	3398
	Uncertainty	373	198	208	56

The anisotropic velocity measurements shows a remarkably velocity increase with the dip (**Figure**). Usually, sedimentary interfaces produce an inverse anisotropy direction (Oberti et al., 1979), indeed waves propagate faster in the horizontal plane of the layers and more slowly perpendicularly through the layers. Here, in our case, highest velocities are observed for sub-vertical rays. However, full range of dips could not be sounded, because of site constrains. The lowest velocity is at a dip of about 35° associated with an azimuth around 220° (**Figure**).

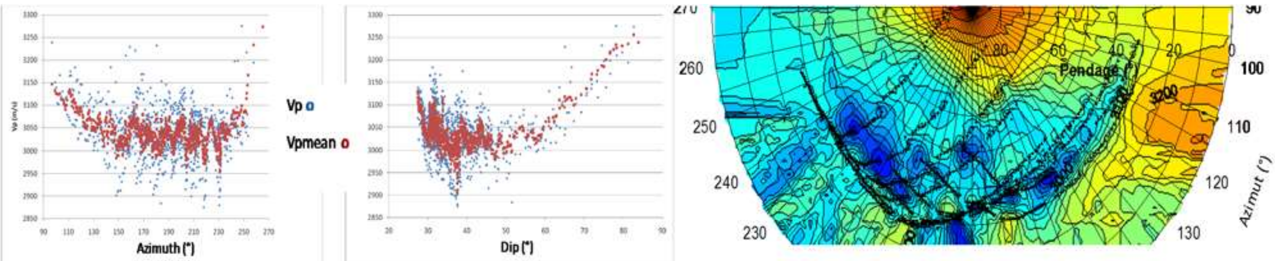

Figure 3 P-wave velocity as a function of azimuth (top), dip (middle) and stereographic representation (bottom).

As for other sites (Ikeda et al., 1981), the origin of this anisotropy is likely to be related with the presence of faults. The NE-SW faults orientation observed underground in the mine (Figure) coincides with the anisotropy velocity field. The most likely hypothesis is that waves which propagate in the fault plane axis encounter "crushed" areas with lower mechanical properties and lower velocities. The influence of faults can also explain the anisotropy inversion due to the stack of sedimentary layers. Without fault on the site, we would probably measure horizontal anisotropy as usually observed in a sedimentary terrain. The effect of faults on velocity is probably underestimated.

3.2 Tomography

The tomography image (Figure) shows a structure of the velocity field that can be divided into three large units that seem to be following the horizontal direction corresponding to the stratigraphy. The first unit located near the sensors has a low velocity (< 2500 m/s) of about 50 m thick. The second unit is 50 to 75 m thick with a high velocity (> 3500 m/s). And the third unit is the most heterogeneous, with velocities of around 3000 m/s.

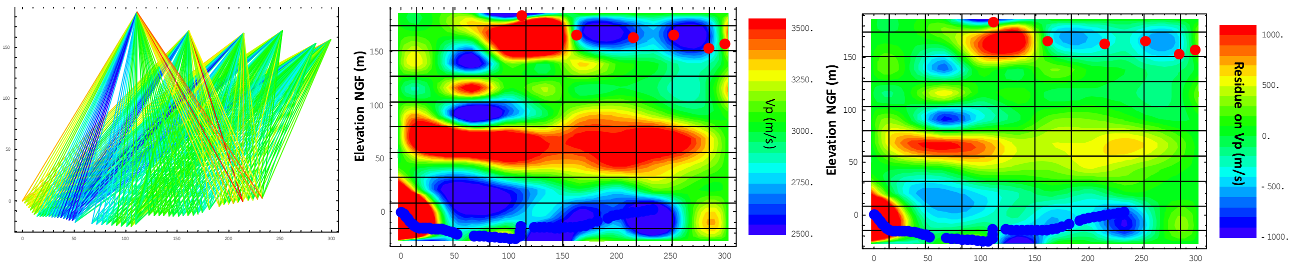

Figure 4 left: 2D seismic ray coverage of the tomographic plan located between shots and streamer 1. Center: tomographic inversion, and right: associated residues. Red points represent the location of the blast and blue points the location of the streamer sensors.

3.3 Sources detectability

The environment of the Groseilliers station has no particularly significant attenuation compared to the Lilas station. This observation is confirmed by the record of an equidistant blast to both stations with maximum amplitude almost identical on both 3 components probes (Figure 5). This shot suggests that the two probes are well coupled to the ground. The minimum explosive source detected by the probes is less than 200 g of explosive at 250 m from a 3 components probe. On the other hand, rockfall on the floor in the gallery Louise (500 kg dropped from 2 m) were detected by Lilas station and this regardless of the hypocentral distance (up to 150 m). Transmission of waves generated by rockfalls is probably advantaged by the strong low-frequency content of the source. The rockfall efficiency must also be better than explosive. Indeed, a significant amount of explosive charge is converted into heat and plastic strain.

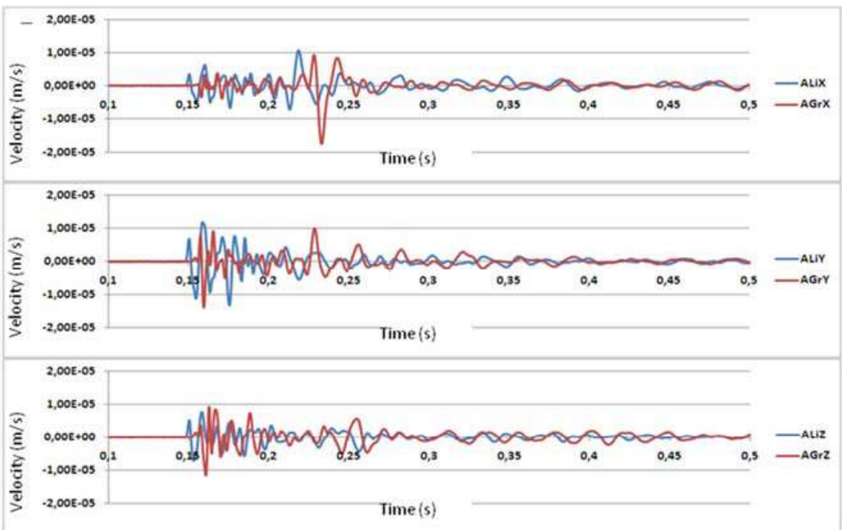

Figure 5 signal representation: (top) X sensor, (middle) Y sensor, and (bottom) Z sensor of a blast (1kg) equidistant from the microseismic stations Lilas and Groseilliers.

3.4 Field attenuation

Signal spectrums of 1DZ and 3DZ seismic sensors of the Lilas station, as well as associated spectrum ratios of weight drops carried out below Lilas station, are showed on Figure . Spectral ratios are quite noisy (Figure -b and d), nevertheless those calculated from the P-wave arrival times are smoother (Figure -d). These spectral ratios show a weak increase of the slope until 250 Hz, and then a decrease. This tendency is clearly visible on the mean spectrum. Several linear regression fittings were tested on spectral ratios in a frequency range between 0 and 250 Hz. From these tests, we observe weak Q factor values. These values are ranging between 5 and 15, because of the data variability (Figure -b and d). Values greater than 20 are likely not possible despite this variability.

Thus, the Q factor for this site can be reasonably estimated at Q = 15 ± 5 on a frequency band ranging between 10 and 250 Hz. These calculations confirm that the anelastic attenuation is significant on the site despite P wave velocities in the order of magnitude of 2900 m/s. In the literature we can observe low Q value factors for velocities between 3000 and 4500 m/s, when the overburden is faulted and fractured (Barton, 2007; Sjogren et al., 1979). Velocities are less sensitive to fracturing of the medium than the Q factor. Indeed, on a site located in similar geological formation (Cerville-Bussoncourt, France), where an underground cavity collapse was triggered, it has been observed that a 10 % velocity change can correspond to a 50 to 70 % variation of the Q factor value (Kinscher, 2015; Marot et al., 2014).

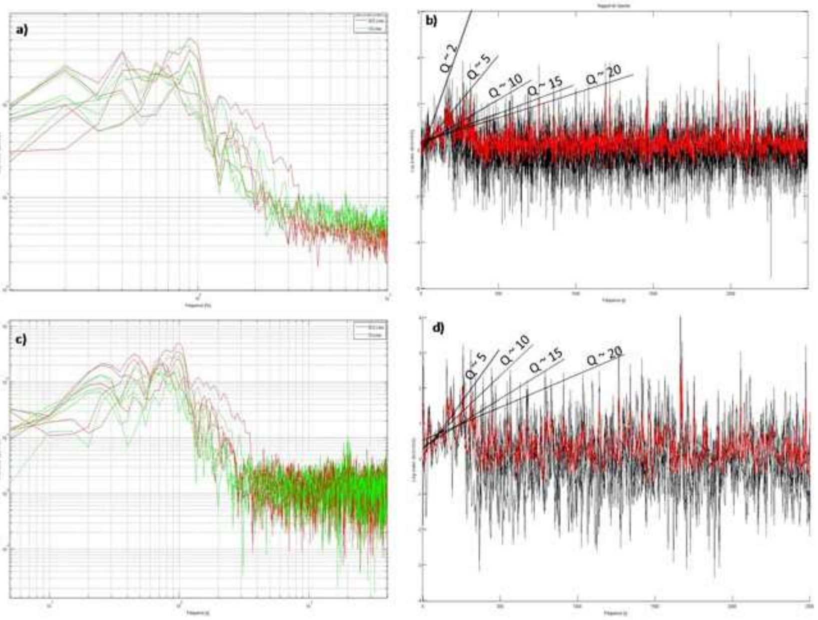

Figure 6 amplitude spectra and spectral ratios of signal from block drops carried out just below the Lilas station, a) considering the entire signal, in green 1DZ sensor and in red 3DZ sensor. b) Spectral ratios with several possible linear regressions and the corresponding Q values, in red average spectrum. c) spectra of the P-wave first arrival and d) associated spectral ratio, in re, average spectrum.

4 Discussion

The low level of seismic signals detected by the Groseilliers station during the subsidence seems to be mainly due to the high seismic attenuation of the site, as shown by this study, as the possibility of a sensor failure is excluded. However, this attenuation phenomenon is likely coupled with very weak seismic sources and/or with very low frequency (< 10Hz). In addition, the collapsed pillars were not probably healthy and may have already been damaged by the old total pillar removal area nearby (robbed pillar area, Figure 14). Moreover the flooding of the area since 2007 has certainly weakened the existing mine workings, because water accelerates crack propagation and thus increases rock damages (GISOS, 2007).

In addition, the uncertainty of the underground galleries positions relatively to the surface, allows considering a location of the maximum surface subsidence from 10 to 30 m further south. This observation could move the collapsed zone in the robbed pillar area, at the border of the healthy gallery. Then, pillars involved in the collapse would have been already damaged by total pillar removal operations, and pillars located nearby have been also fractured. Then the seismogenic (energetic) fracture has certainly occurred prior the installation of the Groseilliers station. We can therefore consider the existence of damaged pillars before the collapse of November 2009. The formation of fractures and/or microcracking in the volume of the pillar would produce a rheology capable of inhibiting large, fast and energetic seismic ruptures. This rheology only would allow slow transient deformation (aseismic slip on fracture planes, and or plastic behavior in the volume), possibly with small seismogenic ruptures, infra-metric, so too weak to be recorded by the Groseilliers station.

Moreover, secondary faults, to the main fault, have been identified in mine workings at the N-W and S-W below the Groseilliers stations (Figure). These faults may have been remobilized during robbed pillar operation of the exploitation located at the SW of the Groseilliers station. This damage zone may also prevent the transmission of the seismic wave generated by subsidence. Therefore the subsidence occurred in areas that already had low mechanical properties due to the robbed pillar extraction method or located inside the area, aggravated by flooding. In addition, many faults have been observed on the site. This causes strong anelastic seismic attenuation, which is not favourable for seismic signal transmission. Figure resume all the hypothesis mentioned in the discussion.

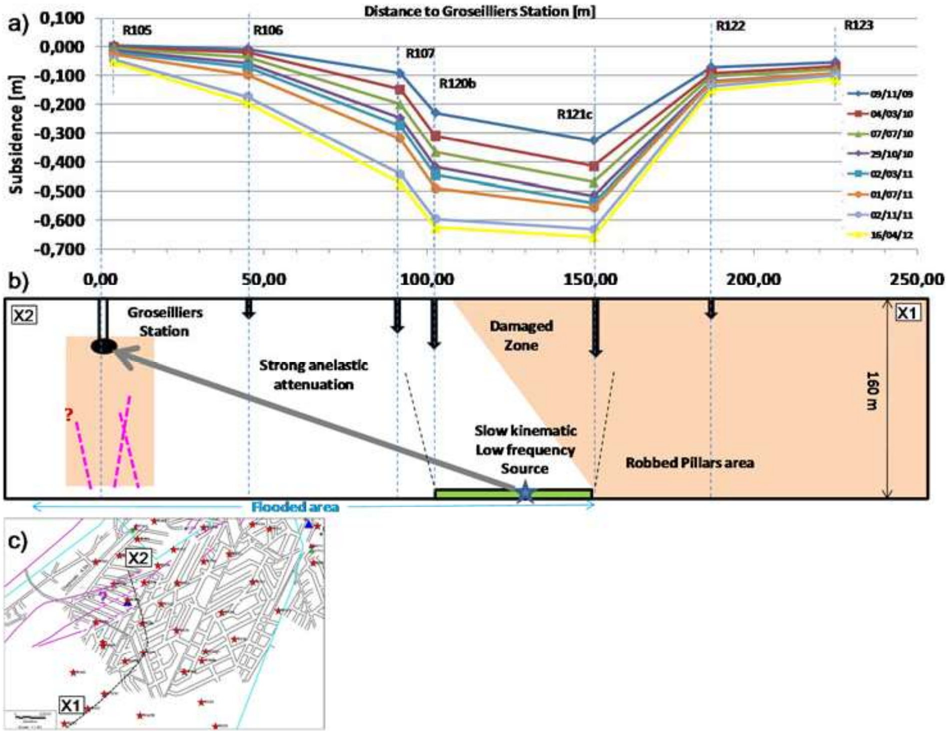

Figure 7 **summary of the hypothesis to explain the lack of detection of the seismic precursory of the subsidence. a) subsidence profile of points along a cross section located between X1 and X2 of the c) figure. b) schematic cross section between X1 and X2 and interpretation.**

5 Conclusions

These investigations helped to highlight an apparent attenuation of the mine overburden, both in terms of intrinsic characteristics. This strong reduction is probably related to the extensive faulting that intersect the mine. This attenuation could explain the non-detection of microseismic events of low energy related to the long term subsidence observed by levelling. Subsidence showed a quasi-linear rate between November 2009 and August 2011, where the average velocity of 2 cm / month. This indicates a slow and steady release of the seismic energy. If, as it was the case for brutal subsidence which occur in 1996 and 1997 at Moutiers and Auboué sites, where most of the energy (about 70 to 80%) was released during few weeks, microseismic events would normally have been recorded. The microseismic monitoring network deployed in the Lorraine iron ore basin is rather design for the detection of rapid subsidence mechanisms. Following this experiment, a differential GPS was installed on the site to follow this progressive subsidence, as it is done for seismological monitoring based on both seismic and geodetic networks.

Acknowledgement

This work was undertaken with the financial support of the French Geological Survey (BRGM-DPSM) upon request of the Regional Direction of Environment, Land Settlement and Housing (DREAL) and the Public Interest Group for support and expert studies (GEODERIS). We thank BRGM-DPSM for making available the technical and human resources involved, without which this large-scale scientific experiment could not have taken place. The authors also thank GEODERIS for their collaboration.

References

Balland, C., Morel, J., Armand, G. and Pettitt, W., 2009. Ultrasonic velocity survey in Callovo-Oxfordian argillaceous rock during shaft excavation. International Journal of Rock Mechanics and Mining Sciences, 46(1): 69-79.

Barton, N., 2007. Rock Quality, Seismic Velocity, Attenuation and Anisotropy. Taylor & Francis, 729 pp.

Bennani, M., Josien, J.-P. and Bigarré, P., 2003. Surveillance des risques d'effondrement dans l'après-mine, besoins, méthodes, Après-mines 2003, Nancy.

Contrucci, I., Klein, E., Bigarré, P., Lizeur, A., Lomax, A. and Bennani, M., 2010. Management of Post-mining Large-scale Ground Failures: Blast Swarms Field Experiment for Calibration of Permanent Microseismic Early-warning Systems. Pure and Applied Geophysics, 167(1-2): 43-62.

Couffin, S., Bigarré, P., Bennani, M. and Josien, J.P., 2003. Permanent real time microseismic monitoring of abandoned mines for public safety. In: M. Frank and T. Francis (Editors), Field Measurements in Geomechanics. Proceedings of the 6th International Symposium, Oslo, Norway, , pp. 437-444.

Deck, O., 2002. Etude des conséquences des affaissements miniers sur le bâti. Propositions pour une méthodologie d'évaluation de la vulnérabilité du bâti, Lorraine, Nancy, 242 pp.

Didier, C., 2007. La politique française de prévention des risques liés à l'après-mine. RÉALITÉS INDUSTRIELLES 86-97.

GISOS, 2007. Synthèse des travaux de recherche après-mine Fer, http://gisos.ensg.inpl-nancy.fr/fileadmin/File/Rapports_synthese/GISOS%20synth%20fer%202007_c.pdf.

Ikeda, K., Ohshima, H. and Sakurai, T., 1981. The property and the seismic wave velocity of fractured zone, Proceeding of International Symposium. on Weak Rock, Tokyo, pp. 527-532.

Kinscher, J., 2015. The analysis and interpretation of microseismicity induced by a collapsing solution mining cavity, thèse de doctorat, Université de Lorraine.

Marot, M., Kinscher, J., Coccia, S., Contrucci, I., Klein, E. and Bigarré, P., 2014. Mine Induced Seismicity: From a Passive Microseismic Monitoring in Complex Near-Field Underground Conditions to an Open & Accessible Database, Fifth EAGE Passive Seismic Workshop.

Oberti, G., Carabelli, E., Goffi, L. and Rossi, P.P., 1979. Study of an orthotropic rock mass: experimental techniques, comparative analysis of results, Proc. of 4th IRSM, Montreux.

Sain, K., Singh, A.K., Thakur, N.K. and Khanna, R., 2009. Seismic quality factor observations for gas-hydrate-bearing sediments on the western margin of India. Marine Geophysical Researches, 30(3): 137-145.

Senfaute, G., Abdul Wahed, M., Piguet, J.-P. and Josien, J.-P., 2000. Technique d'écoute microsismique appliquée au risque d'effondrement dans les mines du bassin ferrifère lorrain. Revue Française de Géotechnique, 92: 57-62.

Sjogren, B., Ofsthus, A. and Sandberg, J., 1979. Seismic classification of rock mas qualities. Geophysical Prospecting, 27: 409-442.

Tastet, J., Contrucci, I., Klein, E., Bigarré, P. and Driad-Lebeau, L., 2007. Large-scale field experiment to calibrate microseismic source parameters applied to realtime monitoring of post-mining instabilities, 11th congress of the international society for rock mechanics, Lisbon, Portugal.

Toksoz, M.N., Johnston, D.H. and Timur, A., 1979. Attenuation of Seismic-Waves in Dry and Saturated Rocks .1. Laboratory Measurements. Geophysics, 44(4): 681-690.